CHARACTERISTICS OF WAVE FIELD GENERATED WHEN WAVES PENETRATE HIGH-VELOCITY LAYERS NEAR THE CRITICAL ANGLE

G. V. GOLIKOVA, M. V. CHIZHOVA and Yu. A. SURKOV[*]

The results obtained from interpreting the wave field of a 1 km offset VSP recorded in a well beneath a high-velocity layer are presented. It was proved that if the angle of incidence of the direct wave was close to the critical angle, the direct wave splits into two components: a ray-type direct wave, which penetrates the layer as a sliding wave, and a screened wave. The screened wave was recorded together with the converted *PSP*-wave at some distance from the first break. In the interpretation, polarization and dynamic features of the waves were used as well as theoretical computations both for the ray-type and the non-ray-type parts of the field.

Keywords: direct wave, converted waves, high-velocity layer, screen, wave field, VSP

1. Introduction

In seismic prospecting practice it was noticed that, when the angle of incidence of the seismic waves arriving to thin, high-velocity layers exceeds the critical angle, seismic energy penetrates the layer whereupon subscreen reflected and refracted waves form in the deeper levels of the stratigraphic sequence contrary to the laws of geometrical optics. GAMBURTSEV [1942] assumed that with increasing offset one meets the phenomenon of screening — which is known in other areas of physics as the 'tunnel effect'. Experimental studies of the screening phenomenon and interpretation of real wave fields in numerous areas of the USSR have resulted in the finding that when high-velocity carbonate rocks are present in the upper levels of the stratigraphic sequence, strong subscreen refracted and reflected waves are detectable. When observing such waves in the immediate neighbourhood of thin layers during vertical seismic profiling one can state that these waves are much more intense than waves which reach the same observation point and propagate in accordance with the laws of geometrical optics.

2. Investigation goals

Experimental vertical seismic profiling was carried out in a borehole — at depths down to 2750 m — with a three-component sonde and a series of shotpoints (SP) of various offsets [GOLIKOVA et al. 1982].

One of the tasks of the investigation consisted in studying the nature of the waves in a wide range of offset (from standard CDP to refraction seismic offsets).

Even while the work was carried out it became obvious that the solution is closely connected with the conditions of the penetration of waves through high-velocity layers.

When analysing and interpreting wave fields we noticed that the phenomena of screening and sliding strongly influence the resulting wave field. In the further discussion, screening will be understood as non-ray-type penetration of a wave through a high-velocity layer when the angle of incidence exceeds the critical angle. Sliding takes place if the angle of incidence is somewhat smaller than the critical angle.

It is usually considered that screening appears at large-offset CDP technique when the reflected wave field is registered in a 1.0–2.5 km range. This is, however, not always true. By VSP it was shown that high-velocity layers in upper levels of the stratigraphic sequence already behave as screens when the offset reaches 0.5 km. With increasing offset, layers lying deeper and deeper turn into screens. For example, high-velocity layers at 2–3 km depths start behaving as screens from a 1.5 km offset. Moreover, it was noted that the offset at which sliding and screening appear also depends on structural features of the sequence. Consequently, sliding waves and screened waves in a seismic wave field are to be expected not only at large-offsets but also at small-offset CDP as well as in parameters of the stratigraphic sequence are highly variable.

In our example there are many high-velocity layers *(Fig. 1.)*. The strongest velocity- and density contrasts are observable on the boundaries of a limestone layer between 360 and 460 m and of anhydrite layers from 2420 to 2460 m and from 2525 to 2550 m depths. The first calculations for direct, refleted and refracted waves for this sequence [GOLIKOVA and CHIZHOVA 1981] were those on screened wave fields in the borehole. In addition, the available published works [FAYZULIN 1971, POGONYAILO 1968] provided data on the screening effect both for field experiments and modelling. In spite of this information, for a long time there was no success in realizing and interpreting the characteristics of the wave field which accompanies the penetration of high-velocity layers at angles close to the critical angle. In the present paper it is described what we could reach in establishing the conditions of screening.

3. Characteristics of the wave field. Interpretation

Let us consider the wave fields of 0.2 s duration after the first break from 645 to 1300 m depths obtained with 1 km (SP–1, *Fig. 2*) and 0.1 km offsets (SP–0, *Fig. 3*), respectively. It can be seen that the wave fields were recorded beneath the limestone layer.

From simple geometrical considerations it can be concluded that for waves SP–1 the angle of incidence of the direct wave and its satellites exceeds 20° whereas from SP–0 the layers are penetrated almost vertically.
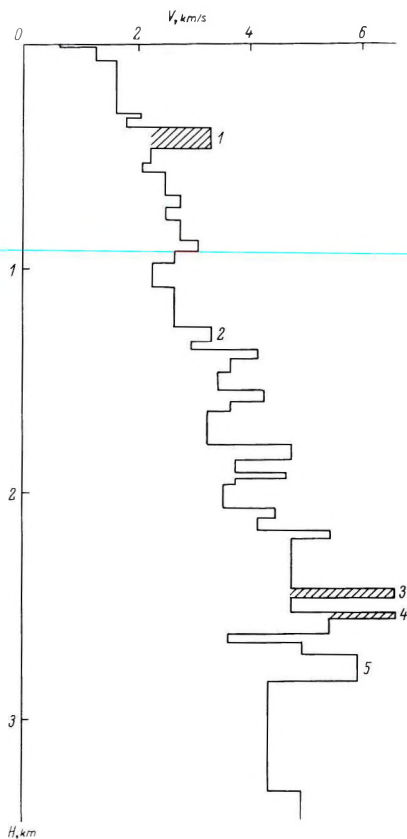
Fig. 1. Velocity sequence. Hatched layers — screens; 1, 2, etc. — serial numbers of high-velocity layers referred to in the paper

1. ábra. Lépcsős sebesség menet. A vonalkázott rétegek az árnyékolók (1, 2 stb. a cikkben használt hivatkozás az egyes árnyékolókra)

Рис. 1. Ступекчатая кривая скоростей. Заштрихованные слои – экраны (1, 2 – ссылки в тексте на номера слоев)

In seismograms from SP–1 (Fig. 2) the direct wave exhibits some peculiarities. In the 645–1000 m depth range it is of lower frequency than it is when deeper. Its amplitude decreases with decreasing depth, i.e. the nearer the observation points are to the screen, which means increasing angle of penetration through the high-velocity layer. At the same time, in the zero-offset seismograms (SP–0, Fig. 3.) the direct wave form is of high stability and decreasing amplitude with increasing depth. Visual study of the seismograms reveals some other differences as well. For example, in the zero-offset records the direct wave sharply attenuates with time, while in the far-offset seismograms after the direct wave arrival a field of nearly the same intensity was recorded. Another peculiarity of the field from (SP–1) is the presence of in-phase axes (hatched peaks) of higher apparent velocities than the direct wave.

In the 1 km offset VSP beneath the high-velocity layer of the above seismograms, in addition to the direct wave and its satellites which originate in the upper levels of the sequence, an intense interference field was recorded consisting of the screened direct wave, E, and converted PSP-waves. This field
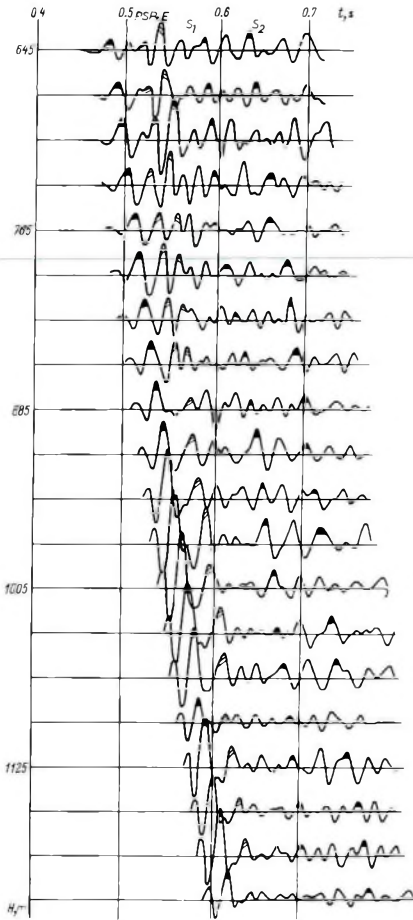
Fig. 2. Records of the Z-component of the VSP field from SP-1. Filled peaks — direct waves and their satellites; hatched peaks — converted *PSP-* and screened waves (*E*)

2. ábra. Az SP-1 robbantópontból kapott VSP hullámtér Z-komponense. Befeketített maximumok a direkt hullámok és szatellitáik, a vonalkázott maximumok a konvertált *PSP-* és az árnyékolt hullám (*E*)

Рис. 2. Компонента Z поля ВСП, полученного из взрывпункта SP-1. Зачерненные экстремумы – падающие волны, заштрихованные экстремумы – волны *PSP* и экранированные (Э).

is observable at depths between 500 and 1300 m. In *Fig. 4* a sketch illustrates the generation of the above-mentioned waves. In order to confirm the above hypothesis experimental and theoretical characteristics of the suggested wave types have been compared. Traveltime curves, amplitude curves of the total displacement vector, and curves of the angle of incidence have been constructed for the phases marked by filled peaks in the seismograms. In general, the quantitative characteristics of the field confirmed its visually detectable features. Let us consider these characteristics in detail.

The direct wave

In *Fig. 5.* amplitude curves for the total displacement vector $A(H)$ are displayed. One of them corresponds to the direct wave in a vertical direction, SP–0 while two others to records of shot points at a distance of 1 km from the
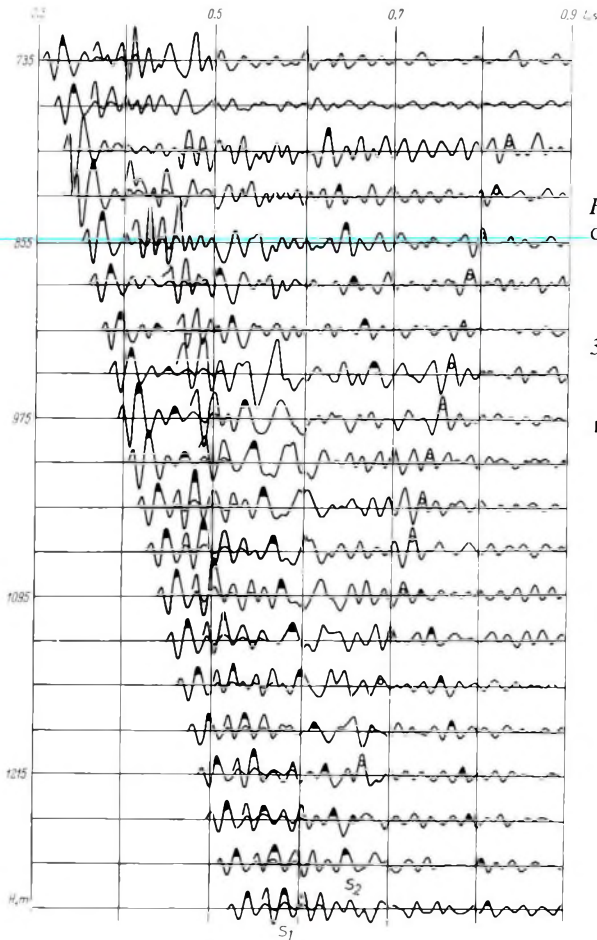
Fig. 3. Record of the Z-component of the VSP field from SP–0. Filled peaks — direct waves and their satellites; peaks with circles — reflected waves

3. ábra. Az SP–0 robbantópontból kapott VSP hullámtér Z-komponense. Befeketített maximumok a direkt hullámok és szatellitáik, a körökkel jelölt maximumok reflektált hullámok

Рис. 3. Компонента Z поля ВСП, полученного из взрывпункта SP–0. Зачененные экстремумы – падающие волны; экстремумы с кружками – отраженные волны.

borehole: SP–1 and SP+1. On the first curve a continuous decrease of the direct wave is observable with increasing depth of the observation points. The behaviour of the curves from SP–1 and from SP+1 is completely different. An interval of sharp increase of the amplitudes can be distinguished from the bottom of the high-velocity limestone layer down to 700 m depth which is replaced by an interval of a less sharp increase of the amplitude between 700 and 1000 m. Further, down to 1500 m the direct wave diminishes a little. At the same time the apparent frequency of the arrivals in the 500–1300 m depth range gradually increases from 30 to 45 Hz.

Polarization diagrams, constructed in the incidence plane by use of a three-component record of the direct wave in the study interval of the sequence, are elliptical with excentricity ($K=1-b/a$) of about 0.8–0.9 (a and b are the

232   *Golikova–Chizhova–Surkov*
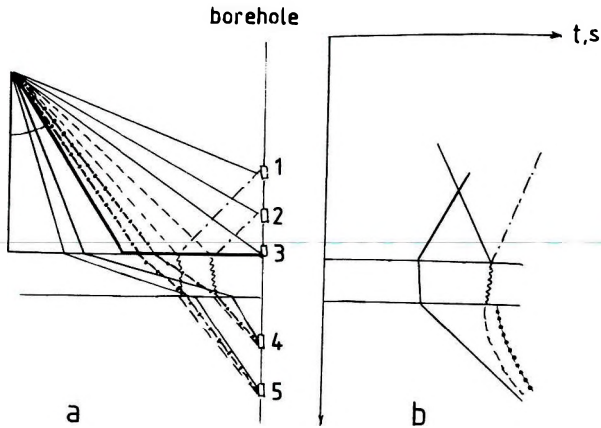

Fig. 4. Sketch of an offset VSP in a model containing a high-velocity layer
a) Sketch of raypaths
b) Traveltime curves
Thin continuous line — direct *P*-wave; dashed line — screened wave; bold dot-dash
line — converted *PSP*-wave; bold-face line — head wave; thin dot-dash line — reflected wave;
1, 2 ... — observation points in the borehole

4. ábra. Távoli gerjesztésű VSP vázlata árnyékolót tartalmazó modell esetén
a) Sugárutak
b) Út–idő görbék
folyamatos vonal — direkt hullám; szaggatott vonal — árnyékolt hullám; vastag pont-
vonal — konvertált *PSP* hullám; vastag folytonos vonal — refraktált hullám; vékony pont-
vonal — reflektált hullám; 1, 2 ... — észlelési pontok a fúrásban

Рис. 4. Схема ВСП с дальним возбуждением для модели с экраном.
а) лучевая схема,
в) годографы.
Сплошные линии – лучи прямой волны; штрихованные линии – лучи
экранированной волны; жирные линии с точками – лучи обменной
волны *PSP*; жирная линия – путь головной волны;
тонкая штрих-пунктирная линия – лучи отраженной волны;
1, 2... – точки наблюдения в скважине.

lengths of the axes of the ellipse). It should be noted that in the deeper levels of
the sequence the excentricity of the first break is as much as 0.95 which means
near-linear polarization. In that the polarization is elliptical. It may support either
interference of the waves or the existence of a wave field which cannot be
described by zero-approximation of the ray-tracing method. For the wave above,
the angles and azimuths of incidence to the observation points have also been
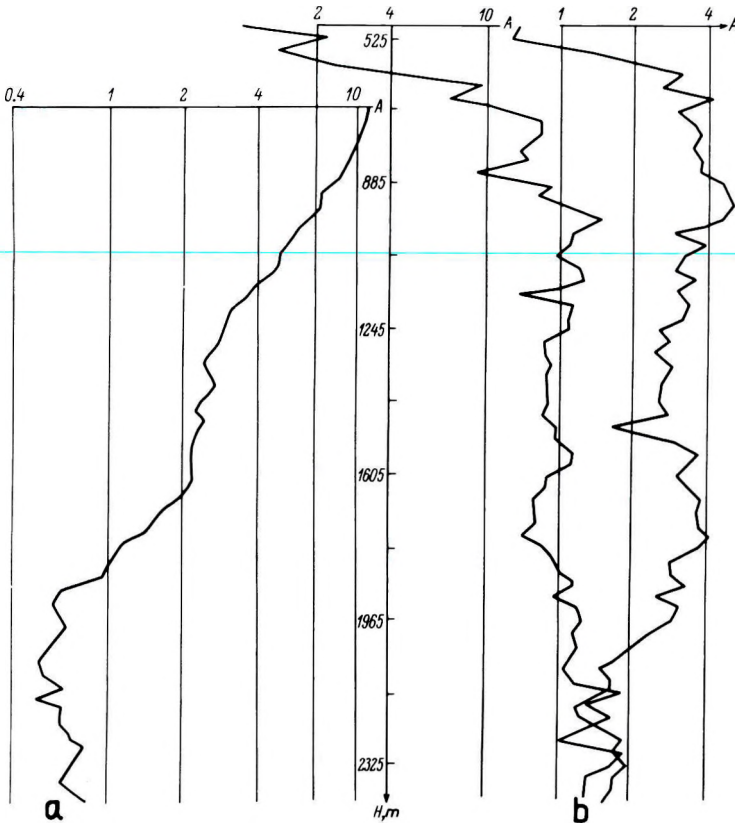computed.

Fig. 5. Amplitude curves of the direct wave

5. ábra. A direkt hullám amplitudó menete

Рис. 5. Амплитудные кривые прямой волны.

Polarization processing of data of three-component VSPs is described by BERDENNIKOVA et al. [1983]. It is known that the parameters of the ray at the observation point can only be determined for the linearly polarized wave from its amplitude. In spite of this, angles of arrival γ for all waves studied have been computed by considering the direction of the large axis of the ellipse as that of the ray. The computed values contain large errors, which exceed 10°. In view of the lack of accuracy in determining the angles of arrival in the interpretation, we have used only a mean value of γ for the whole depth interval under consideration.

Based on computed values of γ we have evaluated the mean angle of arrival of the rays to the upper boundary of the layer. Computations revealed that the angle of incidence of rays of the direct wave is close to the critical angle and that, inside the layer, the wave propagates along sliding trajectories.

It is known that if thin, high-velocity layers are penetrated by sliding waves an interference wave field is generated. Its description is possible by first and higher order approximations of the ray-tracing method. It is suggested that the presence of low frequencies in the record of the direct wave is connected with the mechanism of its penetration through the high-velocity layer and with the existence of displacement components which can be described by the first approximation of wave splitting.

Satellites of the direct wave

In the seismogram of Fig. 3 in the 0.2 s time interval after the first break of the direct wave, a series of in-phase axes of waves parallel to the direct wave is displayed, with an intensity of about 20–30% of that of the direct wave. These waves were generated in the upper levels of the sequence. The relative intensities of the satellites (S_1 and S_2) increase with increasing offset (compare Figs. 2 and 3).

The curves of the angle of incidence versus depth (*Fig. 6*) show a large scatter of local values. The mean values of the angles of incidence lead us to suppose that the satellites, as well as the direct wave, penetrate the high-velocity layer as sliding waves.
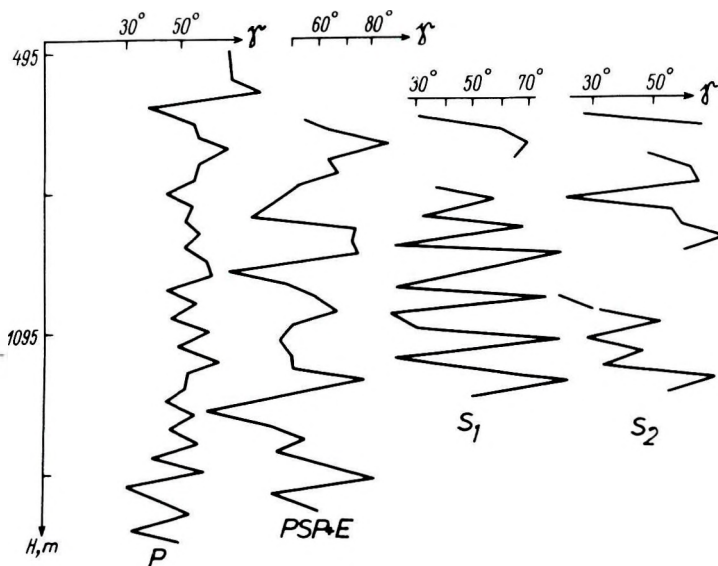

Fig. 6. Angles of arrival versus depth of waves arriving to the observation points from SP-1

6. ábra. A hullámok beérkezési szögei a mélység függvényében
(gerjesztés SP-1-ben)

Рис. 6. Углы подхода волн к точкам наблюдения как функция глубины
(возбуждение в SP-1.).

At large offsets an interference field of unknown origin was recorded between the direct wave and satellites S_1 and S_2. Calculations for the wave kinematics have shown that within this time interval the waves penetrated the high-velocity layer as *PSP*- and screened direct *S*-waves. The behaviour of the computed traveltime curves is in agreement with recorded kinematic data *(Fig. 7)*. *Figure 8* presents the amplitude versus depth curves of this field down to about 1100 m depth. The field intensity sharply decreases below this depth; this sharp decrease is possibly linked with the disappearance of the screened wave and a decrease in the *PSP*-wave intensity. Mean values of angles of arrival of the same phase are of about 55–60° (Fig. 6) and show that, in the wave field, waves are present which were generated at the incidence of the direct wave to the high-velocity layer at angles larger than the critical angle. When considering kinematic and polarization-dynamic characteristics of the wave field originating from SP–1 and recorded beneath the high-velocity layer, we can draw conclusions as follows:
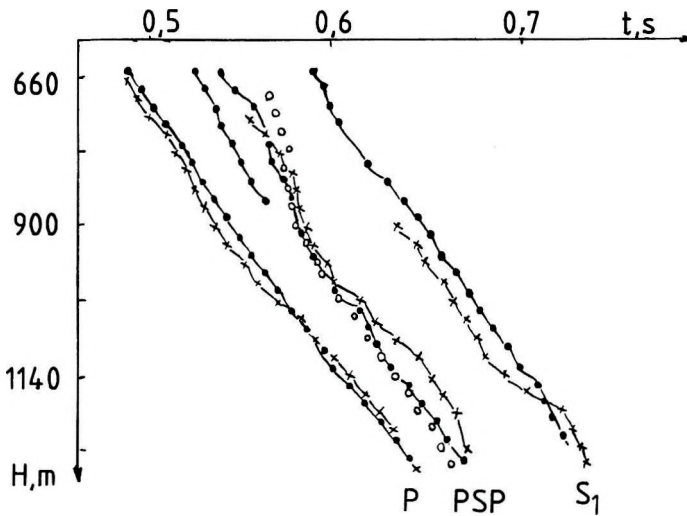

Fig. 7. Traveltime curves of satellite waves of Fig. 2. Lines with dots — recorded peaks; lines with crosses — computed; circles — computed traveltime curve of the screened wave

7. ábra. A 2. ábra hullámainak út–idő görbéi. Pontozott vonal — észlelt maximumok; x-el jelölt vonal — számított görbe; körökkel jelölt vonal — az árnyékolt hullám számított út–idő görbéje

Рис. 7. Годографы волн, регистрируемых вблизи прямой волны рис. 2.
Линии с точками – наблюденные максимумы,
линии с крестиками – расчетные кривые,
кружочки – теоретический годограф экранированной волны.

1) If the angle of incidence of the direct wave arriving to the high-velocity layer is close to the critical angle the wave field splits into two parts. One of them is of ray type and consists of the direct wave proper and its satellites which penetrate the high-velocity layer along sliding rays. The other part propagates through the layer in a non-ray way as a screened wave. Among these waves a converted *PSP*-wave has also been recorded, its role in the wave field increasing if the angle of incidence of the direct wave exceeds the critical.

2) Immediately below the high-velocity layer the whole wave field is of low intensity. With increasing distance from the layer the field intensity sharply increases, with the maximum amplitudes being recorded in the 700–1200 m depth range.

3) Beneath the high-velocity layer the frequency of some waves is decreased.
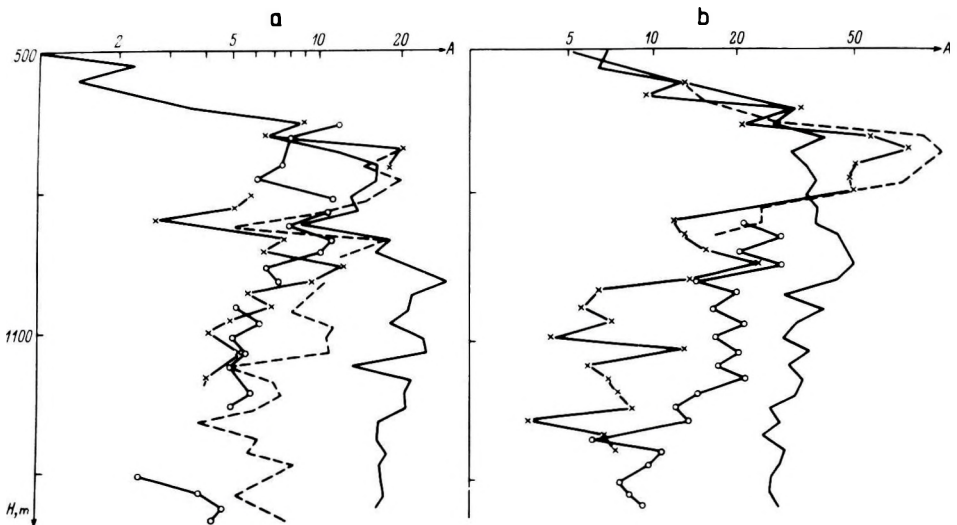

Fig. 8. Experimental amplitude curves for shotpoints SP–1 (a) and SP+1 (b). Continuous line — direct P-wave; dashed line — *PSP*- and screened waves; line with crosses — S_1; line with circles — S_2

8. ábra. Az SP–1-hez (a) és az SP+1-hez (b) tartozó kísérleti amplitudó görbék. Folytonos vonal — direkt P-hullám; szaggatott vonal — *PSP*- és árnyékolt hullám; x-el jelölt vonal — S_1; körökkel jelzett vonal — S_2

Рис. 8. Экспериментальные амплитудные кривые, относящиеся к SP–1 (a) и SP+1 (b). Сплошная линия - прямая волна P; штриховая линия - волные PSP и Э; линия с крестиками - S_1, линия с кружками - S_2.

4. Theoretical wave calculations

In order to confirm the interpretation, those results of theoretical calculations were used which are based on formulae of the zero-approximation of the ray-tracing method. In computations of the screened wave it was taken into account [VORONIN 1959] that the wave attenuation is of exponential type with a factor $\mu\kappa$ where μ = frequency of the recorded wave and κ = screening coefficient.

$$\kappa = h/V \sqrt{\sin^2 \theta - \sin^2 \tilde{\theta}}$$

where h = thickness of screening layer, V = velocity in the layer above the screen, θ = angle of incidence of the ray to the upper boundary of the layer, $\tilde{\theta}$ = angle of total reflection.

In order to compute the wave fields the velocity model of the medium (Fig. 1) was applied. For the main screen, i.e. limestone in the upper level of the sequence, several versions of seismic models were considered. In each model fields of the direct wave, of the screened wave and of the *PSP*-wave were computed and compared.

Theoretical calculations revealed the high-degree of sensitivity of the screened wave intensity to variations in the screen thickness and to the contrast in *P*-wave velocity on its boundaries. For instance, in screen models which consist of a 100 m thick layer the screened wave had insignificant intensity compared with other waves. The best correspondence of theoretical results to experimental data has been achieved for a two-layer screen model having the following parameters, with the 40 m thick layer acting as screen:

$$h_1\text{=55 m}, \quad V_{P1}\text{=2600 m/s}, \quad V_{S1}\text{=900 m/s}, \quad \rho_1\text{=2.3 g/cm}^3$$
$$h_2\text{=40 m}, \quad V_{P2}\text{=3800 m/s}, \quad V_{S2}\text{=2000 m/s}, \quad \rho_2\text{=2.5 g/cm}^3$$

Theoretical amplitude curves of principal waves are displayed in *Fig. 9,* and the corresponding seismograms of the total field in *Fig. 10*. It should be noted that theoretical curves manifest the same type of changes with depth as the experimental curves (Fig. 8). In both of them, the field intensity increases with the distance from the bottom of the screen and with approaching the spot of recording the direct wave at 1000–1200 m depth. Immediately below the screen layer the *PSP*-wave is the most intense. In the model, the intensity of the screened wave is close to that of the direct sliding wave somewhere in the 900–1200 m interval. Precisely in this interval, screened wave kinematics does not differ from that of the direct wave, and together they generate an intense field. At short distances from the layer, the screened wave is of insignificant intensity. Consequently the characteristics of this wave do not allow its independent detection in a seismogram.
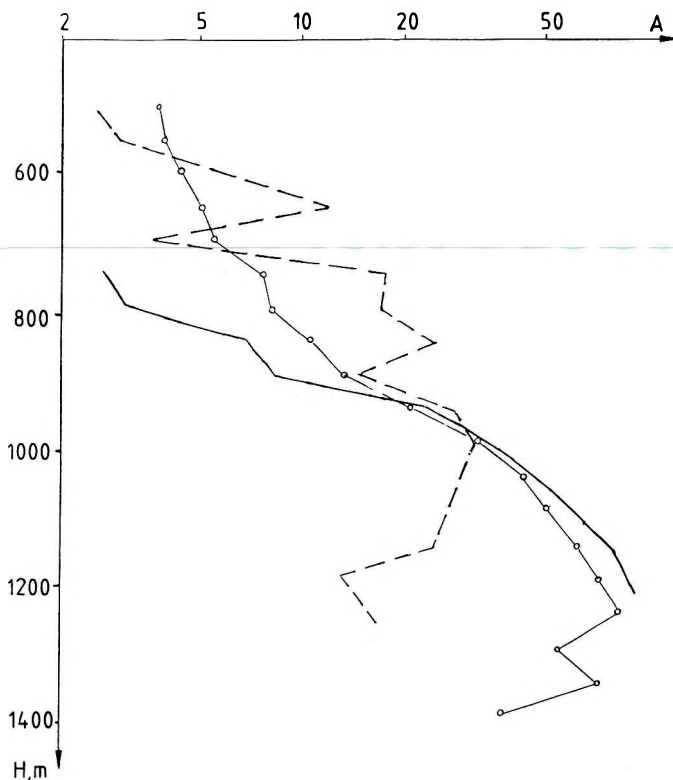
Fig. 9. Theoretical amplitude curves. Continuous line — direct *P*-wave; dashed line — *PSP*-wave; line with circles — screened wave

9. ábra. Elméleti amplitudó görbék. Folytonos vonal — direkt *P*-hullám; szaggatott vonal — *PSP*-hullám; körökkel jelölt vonal — árnyékolt hullám

Рис. 9. Теоретические амплитудные волн.
Сплосная линия – прямая волна *P*; штриховая линия – волна *PSP*;
линия с кружочками – экранированная волна.

    The principal characteristics of the (theoretical and experimental) seismograms are in agreement with each other. A difference, however, can be noted which consists in different depth positions of maximum amplitudes. Attemps to eliminate this lack of agreement by varying the parameters of the high-velocity layer model have not given results. The disagreement between the seismograms is probably connected with the existence of high-velocity layers at depths of 600 and 800 m in the real sequence which are absent in the model.
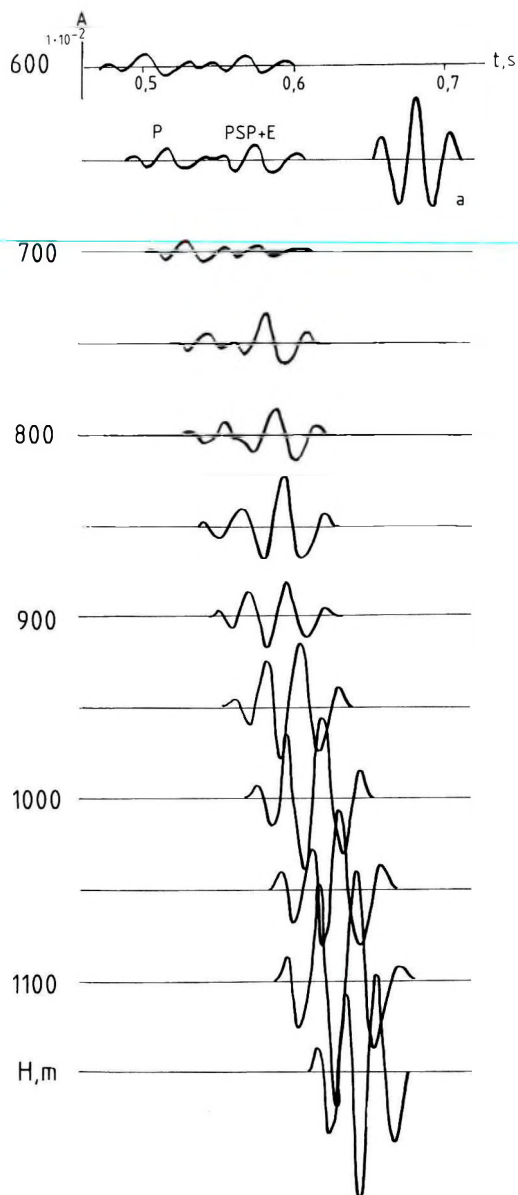
Fig. 10. Theoretical seismogram. a — wavelet used for direct wave

10. ábra. Elméleti szeizmogram. a — a direkt hullámhoz használt elemi jel

Рис. 10. Суммарная теоретическая сейсмограмма. а – форма прямой волны.

These layers may provide additional refraction. The real wave fields are generated by several screens. Moreover, screening and sliding are observable in the fields not only of down-going waves but also of reflected and refracted waves. It is suggested that near the critical angle the field of reflected waves — like that of the direct wave — splits into two parts during penetration through the high-velocity layer, viz. into a ray-type (*PSP*-wave) and a non-ray type part (screened wave). On the surface at a certain offset, one can observe that the reflected wave splits into two waves. The corresponding traveltime curve of the first break of the reflected wave has a higher apparent velocity than that of the second part. Using the model of the study area we calculated traveltime curves of reflected waves taking into account sliding and screening. The results of these calculations allow one to assess the distances at which the splitting into branches of the traveltime curves takes place and the degree of difference between the effective velocities determined from the branches.

Calculations for modelling conventional reflection seismology in a horizontally layered model have also been carried out. As an example, in *Fig. 11* traveltime curves of waves (i) reflected from the boundary of layer 2 in the middle of the sequence (Fig. 1) and (ii) reflected from a deep boundary (layer 5 in Fig. 1) are given. In this case, for one of the reflected waves the limestone layer, 1, is the screen while the corresponding screened wave is generated 1.5 km from the source. The deep reflected wave penetrates anhydrite layers 3 and 4 (Fig. 1) at angles which exceed the critical angle. On the surface, the accompanying screened wave is observable at a distance of 3 km from the source. The traveltime curve of this wave at a distance of 4 km deviates from the first breaks by 40 ms. Thus, in a simple form we can say that the second branch of the traveltime curve appeared. From VSP data, it seems that near the critical angle the intensity of the satellites, the *PSP*-waves and the screened waves brighten up and may generate additional branches of the traveltime curves. The location of this phenomemon may be displaced along the axis depending on the structure.

5. Conclusions

Investigations carried out have shown that if the angle of incidence of the direct wave and its satellites is close to the critical angle, an intense field of secondary waves arises below the high-velocity layer. It has been established that the origin of this field is connected with sliding and screening effects. The principal kinematic and dynamic characteristics of the waves composing the field were investigated. Although the major part of the study is based on VSP data we also used the same velocity model to calculate the moveout of reflected waves in the conventional CDP-technique.
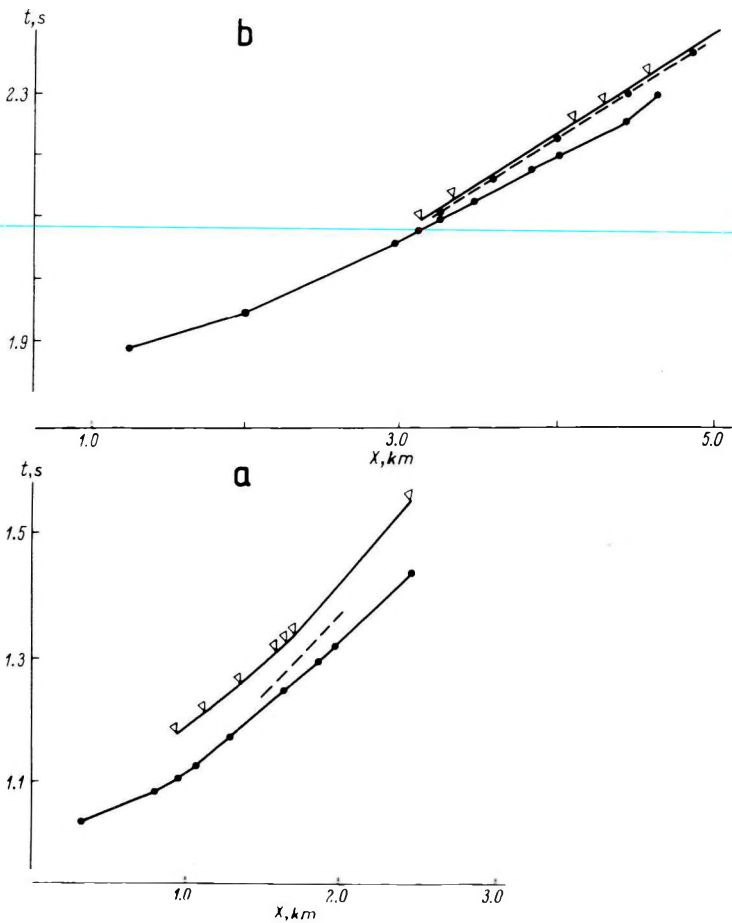
Fig. 11. Modelling of the conventional reflection method: calculated traveltime curves of reflected waves from layer 2 (a) and from layer 5 (b). Line with dots — reflected wave; dashed line — screened wave; line with triangles — *PSP*-wave

11. ábra. A hagyományos reflexiós módszer modellezése: a 2. rétegről reflektált hullámok számított út-idő görbéi (a) és ugyanezek az 5. rétegről (b). Pontokkal jelölt vonal — reflektált hullám; szaggatott vonal — árnyékolt hullám; háromszögekkel jelölt vonal — *PSP*-hullám

Рис. 11. Моделирование традиционного метода отраженных волн.
а) годографы отраженных волн от слоя 2; b) – то же, от слоя 5.
Линия с точками – лучевая отроженная волна;
штриховая – экранированная волна; линия с треугольниками – волна *PSP*.

REFERENCES

BERDENNIKOVA N. I., GOLIKOVA G. V., POGONYAYLO G. G., CHIZHOVA M. V. 1983: The use of polarization- and dynamic characteristics of seismic waves in boreholes (in Russian). Voprosy dinamicheskoy teorii rasprostraneniya seysmicheskikh voln, **XXII**, pp. 168–184

FAYZULLIN I. S. 1971: Modelling of thin high-velocity layers: reflected, refracted and head waves Izv. AN SSSR Fizika Zemli, **8**, pp. 12–22

GAMBURTSEV G. A. 1942: Correlation refraction method (in Russian). Izv. AN. SSSR, ser. geol. i geofiz., **2**, 1–2

GOLIKOVA G. V., BERDENNIKOVA N. I., POGONYAYLO G. G., CHIZHOVA M. V. 1982: The structure of the seismic wave field at different offsets (in Russian). Voprosy dinamicheskoy teorii rasprostraneniya seysmicheskikh voln, **XXII**, pp. 93–97

GOLIKOVA G. V., CHIZHOVA M. V. 1981: The influence of screening phenomena on the kinematics of different types of waves (in Russian). Voprosy dinamicheskoy teorii rasprostraneniya seysmicheskikh voln, **XX**, pp. 119–123

POGONYAYLO G. G. 1968: Study of the wave field in a borehole by offset VSP (in Russian). Voprosy dinamicheskoy teorii rasprostraneniya seysmicheskikh voln, **IX**, pp. 213–235

POGONYAYLO G. G., PETRASHEN G. I., MOLOTKOV L. A. 1974: The influence of thin high-velocity layers in the sedimentary sequence on the reflected wave field at large offsets (in Russian). Voprosy dinamicheskoy teorii rasprostraneniya seysmicheskikh voln, **XXII**, pp. 81–106

VORONIN Yu. A. 1959: Zero offset theoretical seismograms of reflected head- and screened waves (in Russian). Voprosy dinamicheskoy teorii rasprostraneniya seysmicheskikh voln, **III**, pp. 214–251

ÁRNYÉKOLÓ RÉTEG ALATTI HULLÁMTÉR VIZSGÁLATA

G. V. GOLIKOVA, M. V. CSIZSOVA és Ju. A. SZURKOV

1 km robbantási távolságú VSP során, nagy sebességű vékony réteg alatt észlelt hullámtér értelmezését ismertetjük. Bebizonyosodott, hogy ha a direkt hullám beesési szöge a nagy sebességű rétegen a kritikus szöghöz közeli, a direkt hullám két komponensre bomlik: egy sugár típusú direkt hullámra, amely „csúszó" hullámként hatol be a rétegbe, és egy „árnyékolt" hullámra. Ez utóbbit a konvertált *PSP* hullámmal együtt észleljük az első beérkezés után. Az értelmezésben felhasználtuk a hullámok polarizációs és dinamikus tulajdonságait, valamint elméleti számításokat végeztünk a hullámtér sugár-típusú, és nem-sugár-típusú összetevőire.

ОСОБЕННОСТИ ВОЛНОГО ПОЛЯ, ВОЗНИКАЮЩИЕ ПРИ ПРОХОЖДЕНИИ ВЫСОКОСКОРОСТНЫХ СЛОЕВ В ОБЛАСТИ ПРЕДЕЛЬНОГО УГЛА.

Г. В. ГОЛИКОВА, М. В. ЧИЖОВА, Ю. А. СУРКОВ

Приводятся результаты интерпретации волнового поля, зарегистрированного в скважине под слоем высокой скорости при возбуждении из источника, удаленного от устья скважины на один километр. Доказано, что в условиях эксперимента прямая волна падает на слой под углом близким к предельному. При этом она расщепляется на две части: лучевую прямую волну, скользящим образом прошедшую через слой и экранированную. Экранированная волна регистрируется совместно с обменном волной, волной *PSP* на некотором удалении от первых вступлений. Для интерпретации были использованы поляризационно-динамические характеристики волн, а также теоретические расчеты, проводившиеся как для лучевой части поля, так и нелучевой.